NANOMATERIALS SCIENCE & ENGINEERING
Vol. 2, No. 2, pp. 93-98 (2020)

RESEARCH ARTICLE

https://doi.org/10.34624/nmse.v2i2.15737

Crystal structure and magnetic properties of (1-x)BiFeO3 – xBaTiO3 ceramics across the phase boundary

D.V. Zhaludkevich[1*], S.I. Latushka[1], T.V. Latushka[2], A.V. Sysa[3,4], Yu.P. Shaman[3,4], D.A. Dronova[3], A.N. Chobot[1], G.M. Chobot[5], K.N. Nekludov[3], M.V. Silibin[1,3,4,6], D.V. Karpinsky[1,3]

[1] Scientific-Practical Materials Research Centre of NAS of Belarus, 220072 Minsk, Belarus
[2] Belarusian State Medical University, 220116 Minsk, Belarus
[3] National Research University of Electronic Technology "MIET", 124498 Zelenograd, Moscow, Russia
[4]Scientific-Manufacturing Complex "Technological Centre", 124498 Zelenograd, Moscow, Russia
[5] Belarusian State Agrarian Technical University 220023 Minsk, Belarus
[6] Institute for Bionic Technologies and Engineering, I.M. Sechenov First Moscow State Medical University, 119991 Moscow, Russia

**Corresponding author, e-mail address: jeludkevichdima@gmail.com*

Received 7 May 2020; accepted 21 May 2020; published online 10 June 2020

ABSTRACT

The crystal structure and magnetic properties of lead-free ceramics (1-x)$BiFeO_3$ - x$BaTiO_3$ (x < 0.40) prepared by solid state reaction method were studied depending on the chemical composition and temperature. An increase in the concentration of barium and titanium ions leads to the structural transition from the polar rhombohedral structure to the cubic structure through the phase coexistence region characterized by a formation of pseudocubic phase. The isothermal magnetization measurements indicate nearly linear field dependences of magnetization in the temperature range 5 - 300 K which corresponds to a dominance of antiferromagnetic structure in the compounds with x < 0.3. Negligible value of remnant magnetization observed for the compounds having dominant rhombohedral structure diminishes in the compounds with (pseudo) cubic structure. The correlation between the type of structural distortion and magnetic structure is discussed based on the neutron and X-ray diffraction data as well as the magnetization measurements.

1. INTRODUCTION

Materials based on bismuth ferrite attract great attention of the scientific community due to wide variety of structural and magnetic phase transitions [1-10]. While solid solutions based on bismuth ferrite have significant disadvantages - low residual magnetization, high conductivity, small magnitude of magnetoelectric interaction, which significantly limit the scope of their possible applications [8,11-14]. Some of these disadvantages can be overcome using various chemical doping schemes. Thus, chemical substitution of bismuth ions by alkaline-earth elements and substitution of iron ions by other transition metals elements can be used as an effective tool for controlled changes of crystal structure and functional properties [14-19]. The use of alkaline earth ions as dopant ions leads to a significant change in the crystal structure of the compounds, thus the substitution of Ba^{2+} ions having ionic radius larger than that of Bi^{3+} ions causes a stabilization of cubic structure through an intermediate phases [1, 3, 20, 21].

Simultaneous substitution of perovskite lattice in A- and B- positions using alkaline earth ions and transition metals respectively allows to control

the crystal structure of the compounds and to modify their magnetic properties. It is also possible to control the conductivity of the $BiFeO_3$ based compounds and oxygen stoichiometry associated with transport properties [22]. It is known that chemical substitution by barium ions with ions having large ionic radius increases the concentration region of structural stability of the polar rhombohedral phase, and the substitution of iron ions by titanium ions allows to control magnetic properties of the compounds [22, 23].

The present work is focused on the correlation between the crystal structure and magnetic properties of the compounds across the phase transition from the rhombohedral phase to the cubic phase. It is shown that utilizing the mentioned chemical doping scheme allowed to control both electric dipole and magnetic orders in the solid solutions $(1-x)BiFeO_3$ - $xBaTiO_3$, which makes them promising materials to be used in the field of information and energy-saving technologies. The functional materials based on $BiFeO_3$ can be also used as magnetic sensors, capacitive electromagnets, magnetic memory elements, microwave filters and other devices which do not require constant electric currents and associated heat loss.

2. EXPERIMENTAL

Ceramic samples of $Bi_{(1-x)}Ba_xFe_{(1-x)}Ti_xO_3$ system with concentrations of the dopant ions in the range $0.15 \le x \le 0.40$ were prepared by the solid-state reaction method [3,18]. High-purity oxides Bi_2O_3, Fe_2O_3, TiO_2 and carbonite $BaCO_3$ (Sigma-Aldrich, ≥ 99%) taken in stoichiometric ratio were mixed using planetary ball mill (Retsch PM 200). The samples were uniaxially pressed into tablets with a diameter of 10 mm. Preliminary synthesis was performed at 900 °C, after intermittent grinding the samples were finally synthesized at temperatures 910 - 945°C (synthesis temperature was gradually increased with the dopants concentration) [22, 24]. After synthesis the samples were cooled down to room temperature with a cooling rate of 100 °C/h.

X-ray diffraction patterns were recorded in the 2thetta range of 20 - 80° with a step of 0.02° using Bruker D8 Advance and Rigaku D/MAX-B diffractometers with Cu-Kα radiation. Neutron powder diffraction (NPD) measurements were performed using high-resolution neutron powder diffractometer FIREPOD (λ=1.7977Å, E9 instrument, HZB). The diffraction data were analyzed by the Rietveld method using the FullProf software [25]. Magnetization measurements were performed in magnetic fields up to 14 T using physical properties measurement system from Cryogenic Ltd.

3. RESULTS AND DISCUSSIONS

The refinement of the diffraction data obtained for the compounds of the system

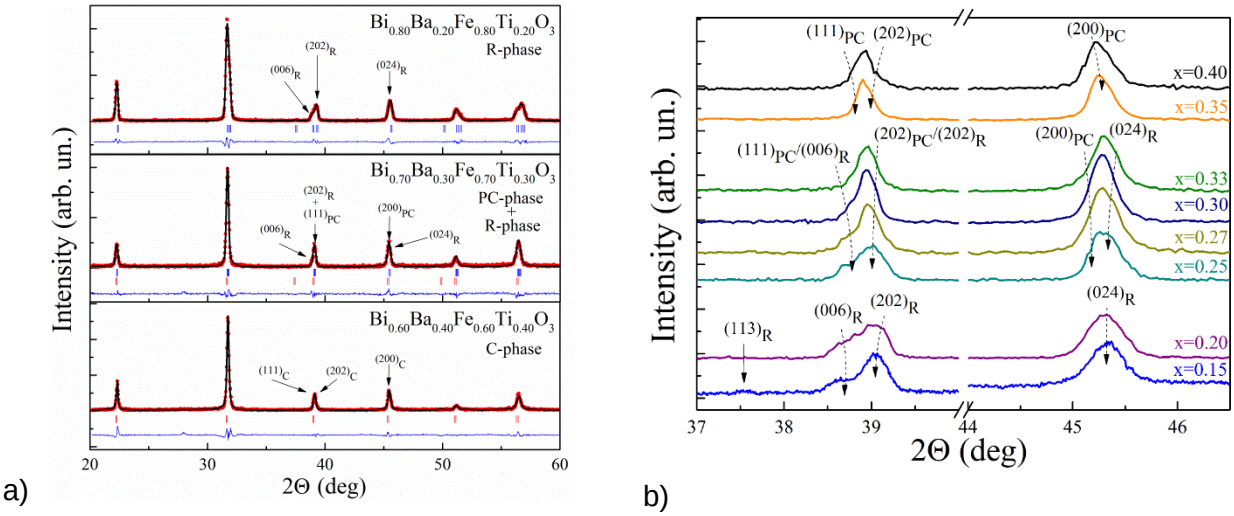

Figure 1. (a) Room-temperature XRD patterns of the compounds $Bi_{(1-x)}Ba_xFe_{(1-x)}Ti_xO_3$ x= 0.20; 0.30; 0.40; observed and calculated profiles are marked by dots and solid line respectively, the line below the pattern refers to the difference between the profiles. The upper row of the ticks denotes Bragg reflections ascribed to the rhombohedral phase, the second row – to the cubic phase; (b) the evolution of the selected diffraction peaks depending on the concentration.

$Bi_{(1-x)}Ba_xFe_{(1-x)}Ti_xO_3$ has allowed to clarify the evolution of the crystal structure as a function of the dopant concentration and temperature. According to the results of the diffraction measurements, the compounds with $x \leq 0.2$ are characterized by a single-phase rhombohedral structure (Fig. 1a,b). An increase in the concentration of the dopant content leads to a reduction of the rhombohedral distortion, and the structure of the compounds with x = 0.25 - 0.33 can be refined assuming a coexistence of the rhombohedral and pseudocubic phases. It should be noted that the pseudocubic phase is observed in the compounds $0.25 < x < 0.40$. This model is in accordance with the results obtained by X-ray and neutron diffraction measurements.

Chemical substitution causes gradual decrease in rhombohedral distortions, which can be estimated by an evolution of the reflection $(113)_R$ (Fig. 1b) associated with a distortion of oxygen octahedra in the *ab* plane of the rhombohedral lattice. The intensity of the reflection gradually decreases with the concentration *x* and disappears for the compound x = 0.2. The splitting of the reflections $(202)_R$ and $(006)_R$ (2Θ = 39 °) characterizing rhombohedral distortion gradually decreases with increasing in the concentration of the dopant ions, which indicates gradual decrease in the elongation of the rhombohedral lattice. This splitting completely disappears for the compound with x = 0.35, which also confirms the absence of the rhombohedral phase in the compounds with $x > 0.35$. Further substitution leads to a transformation of the crystal structure and the structural state becomes to be single phase with cubic symmetry.

Thus, an increase in the concentration of Ba and Ti ions in the compounds $Bi_{(1-x)}Ba_xFe_{(1-x)}Ti_xO_3$ leads to the structural transition from the polar rhombohedral phase to the cubic phase through the formation of an intermediate pseudocubic phase. Chemical substitution leads to an increase in the unit cell volume which is caused by larger ionic radii of the dopant ions as compared to the radii of Bi and Fe ions [26], wherein the *a*- and *c*-parameters of the unit cell change in different ways (Fig. 2). An increase in the unit cell volume is accompanied by a gradual decrease in rhombohedral distortion, and the angle α_R, which describes the rhombohedral distortion, gradually increases from 59.55° for the compound with x = 0.2 to 59.98° for the compound with x = 0.35, the volume fraction the rhombohedral phase in the last compound becomes to be negligible (Fig. 2).

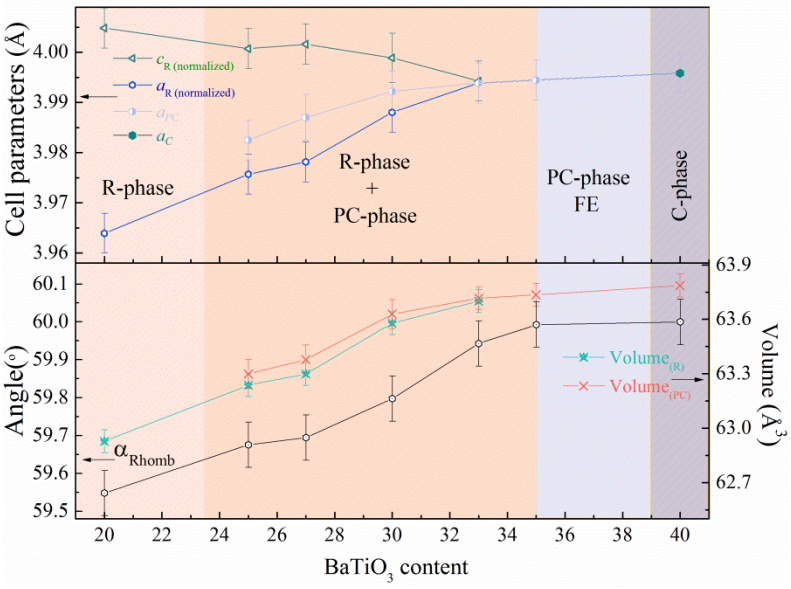

Figure 2. The dopant concentration driven evolution of the unit cell parameters (upper panel), unit cell volume of the rhombohedral and (pseudo)cubic phases and angle α_R calculated for the compounds with $0.2 \leq x \leq 0.4$.

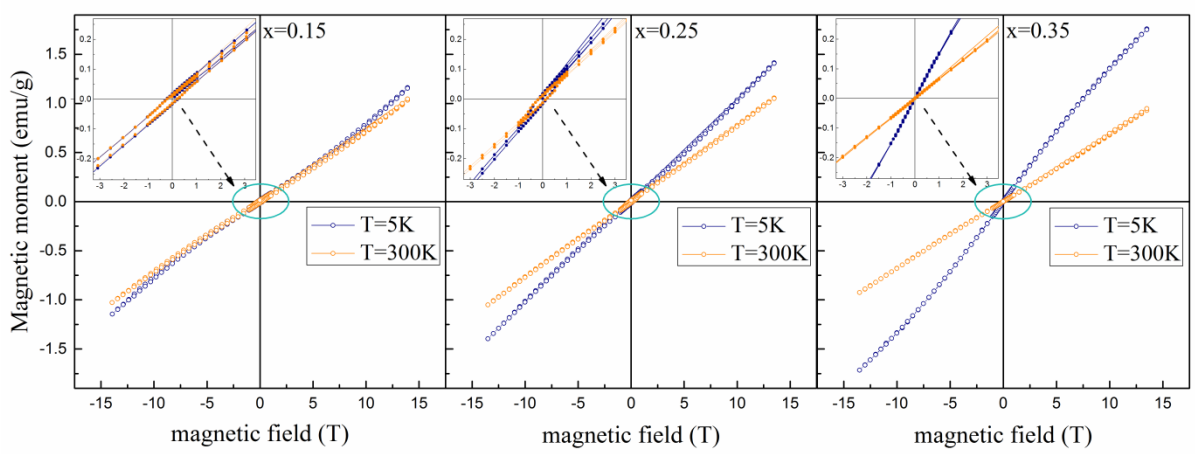

Figure 3. Field dependences of magnetization obtained for $Bi_{(1-x)}Ba_xFe_{(1-x)}Ti_xO_3$ compounds 0.15 ≤ x ≤ 0.40 at temperatures T = 5 K and 300 K. The insets show magnified parts of the magnetization curves near the origin.

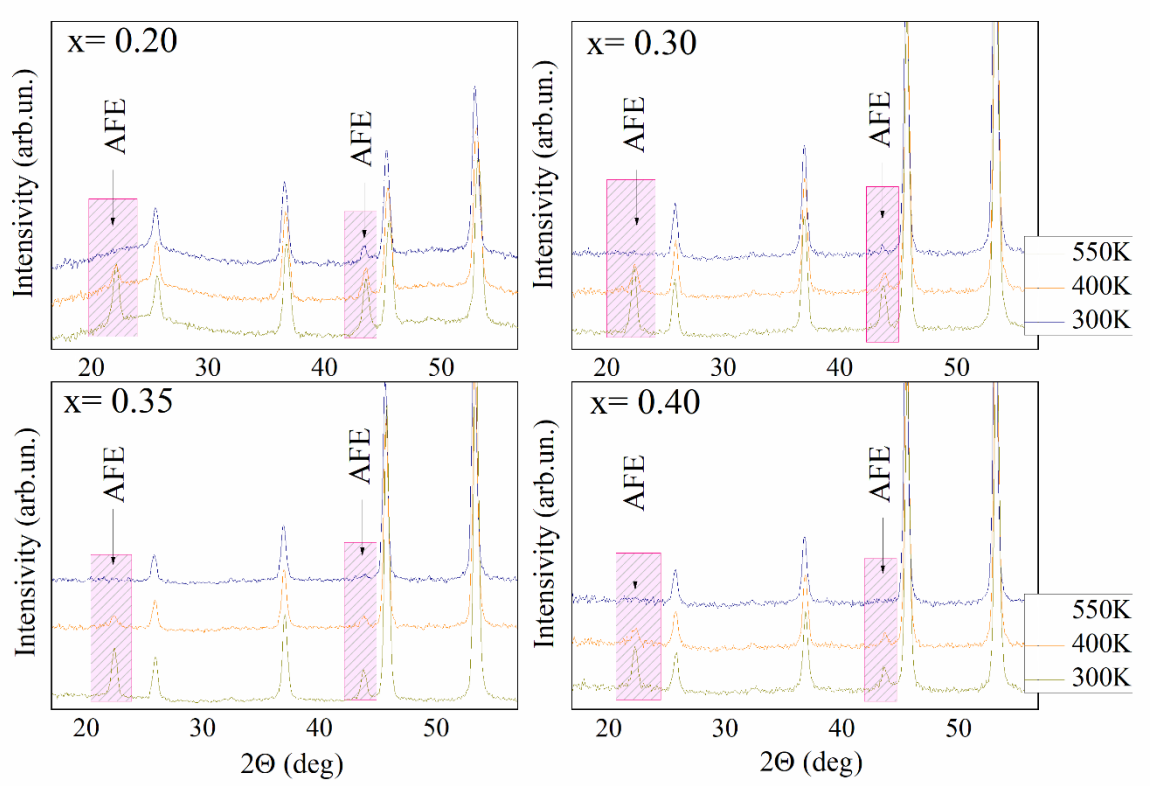

Figure 4. Temperature evolution of characteristic diffraction peaks obtained by neutron diffraction for the compounds $Bi_{1-x}Ba_xFe_{1-x}Ti_xO_3$ with 0.20 ≤ x ≤ 0.40. The diffraction reflections ascribed to magnetic scattering are marked and highlighted by dashed areas.

It should also be noted that the parameter *a*- gradually increases with the dopant content up to x = 0.40, while *c* - parameter begins to significantly decrease only in the compounds with x = 0.27. It should be noted that the *c* / *a* ratio which denotes polar distortion of the lattice decreases down to unity in the compound with x = 0.33.

Magnetization measurements have allowed to reveal a close correlation between the crystal

structure and magnetic properties of the compounds. The M(H) dependence obtained for the compound with x = 0.15 has a residual magnetization of about 0.011 emu/g (Fig. 3, inset) and has slightly non-linear character distinctly observed at low temperature which points at a disruption of spatially modulated spin structure at high magnetic fields. The M(H) dependences obtained for compounds with the dopant content x > 0.15 are characterized by nearly linear character of magnetization denoting dominant antiferromagnetic structure. At x = 0.25, the compound is characterized by a mixture of dominant rhombohedral phase and minor pseudo-cubic phase and the remanent magnetization is still present with a value of about 0.014 emu/g. Increase in the concentration of the dopant ions up to x = 0.30 leads to a complete collapse of remanent magnetization which is valid for the compounds with x ≤ 0.4. Such evolution of magnetization is caused by a change in symmetry of the crystal structure from the rhombohedral to the (pseudo)cubic phase. Magnetization data obtained at room temperature indicate the stability of the antiferromagnetic structure in the studied temperature range and the data are in good agreement with the results obtained by the neutron diffraction measurements.

The results of the magnetization measurements performed for the compounds $Bi_{(1-x)}Ba_xFe_{(1-x)}Ti_xO_3$ indicate predominantly antiferromagnetic character of the magnetic structure, which is confirmed by the results of neutron diffraction measurements which indicate the G-type antiferromagnetic structure. Analyzing the data of the neutron diffraction measurements (Fig. 4), it can be stated that the G-type antiferromagnetic structure is stable in the compounds with 0.15 ≤ x ≤ 0.4 in the temperature range 5 K ≤ T ≤ T_N. At temperatures above room temperature the diffraction peaks attributed to magnetic scattering become to decrease rapidly till they disappear completely at T_N ~ 500 K for the compounds with x = 0.25 – 0.30. Increase in the dopant concentration up to x= 0.40 leads a reduction of the magnetic transition temperature down to T_N ~ 450 K.

Neutron diffraction data points at G-type antiferromagnetic structure which is stable in the compounds $Bi_{(1-x)}Ba_xFe_{(1-x)}Ti_xO_3$ x ≤ 0.40. The magnetic moment calculated per iron ion of the compound with x = 0.15 at room temperature is about 4.5 μ_B which is only a bit lower than “spin only” value of the magnetic moment estimated for the iron ions being in 3+ oxidative state (t_{2g}^5). The nearly collinear antiferromagnetic structure remains in the compounds upon increase in the dopant content while the magnetic moment associated with the iron ions gradually decreases with x. The compound with the dopant content x=0.25 is characterized by the magnetic moment of ~ 4.2 μ_B, for the compound with x = 0.35 the calculated value of the magnetic moment is ~ 2.9 μ_B. The obtained results are in accordance with the model of diamagnetic dilution of the magnetically active sublattice formed by the iron ions being in 3+ oxidative state, while non-magnetic titanium ions are characterized by the oxidative state of 4+. It should be noted that the remanent magnetization observed in the compounds having dominant rhombohedral phase diminishes in the compounds having dominant (pseudo) cubic phase. This observation is in accordance with the symmetry restrictions, as antisymmetric exchange interactions leading to nonzero remanent magnetization in the compounds with rhombohedral structure are forbidden in the compounds having cubic phase [27-29].

4. CONCLUSIONS

The results of diffraction measurements indicate that the single-phase rhombohedral structure is stable in the compounds up to x = 0.2. An increase in the concentration of the dopant content leads to a gradual reduction of the rhombohedral distortion, the structure of the compounds with x = 0.25 - 0.33 can be refined assuming a coexistence of the rhombohedral and pseudocubic phases, further increase in the dopant content leads to the phase transition to single phase cubic structure. Analysis of the isothermal dependences of the magnetization as well as neutron diffraction measurements points at G-type antiferromagnetic structure which is stable in the compounds with 0.15 ≤ x ≤ 0.4 in the wide temperature range in spite of magnetic dilution caused by Ti ions residing in the B-site of perovskite lattice. The obtained results point at

strong correlation between the presence of remanent magnetization and structural state of the compounds, thus confirming weak ferromagnetism specific for the compounds having rhombohedral structure; the absence of remanent magnetization in the compounds having (pseudo) cubic structure is in accordance with symmetry restrictions.

ACKNOWLEDGMENTS

This work was supported by the Russian Science Foundation (project 18-19-00307). The authors acknowledge HZB for the allocation of neutron radiation beamtime and HZB staff for the assistance with neutron diffraction experiments. M.S. acknowledges Russian academic excellence project “5-100” for Sechenov University.

REFERENCES

[1] S. Kim, G.P. Khanal, H.-W. Nam, I. Fujii, S. Ueno, C. Moriyoshi, Y. Kuroiwa, S. Wada, *J. Appl. Phys.* **122,** 164105 (2017).
[2] R. Haumont, I.A. Kornev, S. Lisenkov, L. Bellaiche, J. Kreisel, B. Dkhil, *Phys. Rev. B* **78,** 134108 (2008).
[3] D.V. Karpinsky, I.O. Troyanchuk, M. Tovar, V. Sikolenko, V. Efimov, E. Efimova, V. Ya Shur, A.L. Kholkin, *J. Am. Ceram. Soc.* **97,** 2631-2638 (2014).
[4] D. Wang, G. Wang, S. Murakami, Z. Fan, A. Feteira, D. Zhou, S. Sun, Q. Zhao, I.M. Reaney, *J. Adv. Dielectr.* **08,** 1830004 (35p) (2018).
[5] D.C. Arnold, K.S. Knight, G. Catalan, S.A.T. Redfern, J.F. Scott, P. Lightfoot, F.D. Morrison, *Adv. Funct. Mater.* **20,** 2116-2123 (2010).
[6] A. Kirsch, M.M. Murshed, M.J. Kirkham, A. Huq, F.J. Litterst, T.M. Gesing, *J. Phys. Chem. C* **122**, 28280-28291 (2018).
[7] D. Wang, A. Khesro, S. Murakami, A. Feteira, Q. Zhao, I.M. Reaney, *J. Eur. Ceram. Soc.* **37,** 1857-1860 (2017).
[8] G. Catalan, J.F. Scott, *Adv. Mater.* **21,** 2463-2485 (2009).
[9] S.M. Selbach, T. Tybell, M.-A. Einarsrud, T. Grande, *Adv. Mater.* **20**, 3692-3696 (2008).
[10] D.V. Karpinsky, I.O. Troyanchuk, O.S. Mantytskaya, V.A. Khomchenko, A.L. Kholkin, *Solid State Commun.* **151,** 1686-1689 (2011).
[11] I.O. Troyanchuk, D.V. Karpinsky, M.V. Bushinsky, V.A. Khomchenko, G.N. Kakazei, J.P. Araujo, M. Tovar, V. Sikolenko, V. Efimov, A.L. Kholkin, *Phys. Rev. B* **83**, 054 109 (2011).
[12] G. Le Bras, P. Bonville, D. Colson, A. Forget, N. Genand- Riondet, R. Tourbot. *Physica B* **406**, 1492-1495 (2011).
[13] I. Levin, M.G. Tucker, H. Wu, V. Provenzano, C.L. Dennis, S. Karimi, T. Comyn, T. Stevenson, R.I. Smith, I.M. Reaney. *Chem. Mater.* **23**, 2166-2175 (2011).
[14] D. Kan, L. Palova, V. Anbusathaiah, C.J. Cheng, S. Fujino, V. Nagarajan, K.M. Rabe, I. Takeuchi. *Adv. Funct. Mater.* **20**, 1108-1115 (2010).
[15] D. Arnold, *IEEE Trans. Ultrason. Ferroelectr. Freq. Control* **62,** 62-82 (2015).
[16] D.V. Karpinsky, I.O. Troyanchuk, N.V. Pushkarev, A. Dziaugys, V. Sikolenko, V. Efimov, A.L. Kholkin, *J. Alloy. Comp.* **638,** 429434 (2015).
[17] V.A. Khomchenko, M.S. Ivanov, D.V. Karpinsky, J.A. Paixao, *J. Appl. Phys.* **122,** 124103 (2017).
[18] D.V. Karpinsky, M.V. Silibin, A.V. Trukhanov, A.L. Zhaludkevich, T. Maniecki, W. Maniukiewicz, V. Sikolenko, J.A. Paixao, V.A. Khomchenko, *J. Phys. Chem. Solids* **126,** 164-169 (2019).
[19] L.H. Yin, W.H. Song, X.L. Jiao, W.B. Wu, X.B. Zhu, Z.R. Yang, J.M. Dai, R.L. Zhang, Y.P. Sun, *J. Phys. D Appl. Phys.* **42,** 205402 (2009).
[20] A. Singh, C. Moriyoshi, Y. Kuroiwa, D. Pandey, *Phys. Rev. B* **88,** 024113 (2013).
[21] I. Calisir, A.A. Amirov, A.K. Kleppe, D.A. Hall, *J. Mater. Chem. A* **6,** 5378-5397 (2018).
[22] D.V. Karpinsky, M.V. Silibin, A.V. Trukhanov, A.L. Zhaludkevich, S.I. Latushka, D. V. Zhaludkevich, V. Sikolenko, V.A. Khomchenko, *J. Alloy. Comp.* **803,** 1136-1140 (2019).
[23] V.A. Khomchenko, D.V. Karpinsky, D.V. Zhaludkevich, S.I. Latushka et. al., *Mater. Lett.* **254,** 305 (2019).
[24] Y.P. Wang, L. Zhou, M.F. Zhang, X.Y. Chen, J.-M. Liu, Z.G. Liu, *Appl. Phys. Lett.* **84,**) 1731 (2004.
[25] J. Rodríguez-Carvajal, *Physica B* **192,** 55-69 (1993).
[26] R. D. Shannon, *Acta. Cryst.* **A32,** 751-767 (1976).
[27] I. Dzyaloshinsky, *J. Phys. Chem. Solids* **4**, 241-255 (1958).
[28] T. Moriya, *Phys. Rev. Lett.* **4**, 228 (1960).
[29] T. Moriya, *Phys. Rev.* **120**, 91 (1960).